Radiative Pion Capture in ^{4}He†

Arthur Raiche and Carl Werntz
Physics Department, Catholic University of America, Washington, D. C. 20017

(Received 21 December 1970)

The radiative-pion-capture rate from a number of low-lying Bohr orbits in ^{4}He is calculated. It is shown that the peak in the γ spectrum is caused by transitions to broad 2^- and 1^- resonances in ^{4}He. The angular correlation of the low-energy neutrons with the direction of the γ ray is shown to be strongly dependent on the orbital-angular-momentum value of the Bohr orbit from which capture occurs, thus affording an independent check of atomic deexcitation studies in pionic atoms.

I. INTRODUCTION

The T matrix for the radiative capture of a π^- by a proton takes a very simple form in the low-momentum limit:

$$t(q,k) \cong -ef\frac{1}{m_\pi^{\,2}}\tau^{(-)}\hat{\epsilon}\cdot\sigma\,. \tag{1}$$

Here $e^2/4\pi = \frac{1}{137}$ and $f^2/4\pi = 0.08$ are the electromagnetic and strong-interaction coupling constants. The amplitude describes the transition from an s-wave pion to an $E1$ photon. Since the momenta of a pion in a Bohr orbit around a light nucleus are small, higher-order terms, i.e., p-wave pions and $M1$ photons, contribute at most a few percent[1] to the radiative capture in complex nuclei.

Because of the simplicity of the interaction and the unique signal of the high-energy γ rays, the study of radiative pion capture in nuclei offers certain advantages as compared to a similar interaction, the capture of a μ^- by nuclei. However, complicating factors, especially in the theoretical interpretation, are (1) the necessity of considering the initial-state interaction of the π^- with the nucleus, either by means of an optical model[2] or by multiple-scattering theory,[3] and (2) the necessity of taking a proper average for capture from a number of low-lying Bohr orbits rather than from a single orbit, the $1s$. An experimental complication is the low branching ratio, ~1%, for the radiative capture as compared to the nonradiative capture.

The importance of capture from other than the $1s$ orbit in even the lighest nuclei has been generally underestimated. Published work on radiative pion capture in deuterium[3] and ^{4}He[4] has considered only s-state capture. Likewise, recent calculations of nonradiative capture[5,6] have treated only s-wave capture of the π^- by ^{4}He and ^{6}Li.

Restricting ourselves to ^{4}He, we find that Eisenberg and Kessler[7] in their original cascade calculations estimated that only about 10% of the π^- are captured from the p orbits. Later, Ericson and Figereau[8] quote a figure of 30% for the percentage of p-state captures. The most extensive x-ray yield measurements[9] interpreted by refined cascade calculations give a p/s-state absorption ratio of 1.2 ± 0.3.

A major contribution of the present work is to point out that a particularly simple feature of the nuclear structure of ^{4}He, namely, that $1s$-to-$1p$ transitions of a single nucleon dominate the radiative pion capture, makes possible a determination of the p/s ratio for radiative capture. This ratio, $R_\gamma(p/s)$, is related to the p/s ratio for nonradiative capture $R(p/s)$ through the relations

$$R_\gamma\left(\frac{p}{s}\right) = \sum_n \frac{\Lambda_\gamma(np)}{\Lambda(np)}w_{np}\left[\sum_n \frac{\Lambda_\gamma(ns)}{\Lambda(ns)}w_{ns}\right]^{-1},$$
$$R\left(\frac{p}{s}\right) = \sum_n w_{np}\Big(\sum_n w_{ns}\Big)^{-1}. \tag{2}$$

In the above equation $\Lambda_\gamma(np)$ is the radiative-capture rate from a p state with principal quantum number n, $\Lambda(np)$ is the nonradiative-capture rate from the same orbit, w_{np} is the total percentage of captures from that orbit, and the quantities with ns labels refer to the same objects with reference to s-state Bohr orbits.

II. FORMALISM

By using the impulse approximation the amplitude in Eq. (1) can be used to calculate a differential capture rate for the radiative capture of the π^- from a Bohr orbit. Restricting ourselves to two-body nucleon final states, the differential rate is

$$\frac{d^2\Lambda}{dq\,d\Omega}=\frac{\alpha f^2}{(2\pi)^3}\,\frac{|\vec{q}|\,|\vec{k}|\,\mu}{m_\pi{}^3}\,\frac{1}{1+q/4m}\Big|\langle\psi_f^{(-)}|\sum_{j=1}^{A}\tau_j^{(-)}\vec{\sigma}_j\cdot\vec{\epsilon}^{\,*}e^{-\vec{q}\cdot\vec{r}_j}\varphi_\pi(\vec{r}_j)\,|\,\psi_i\rangle\Big|^2\,. \tag{3}$$

In the above, $\vec{q}$ is the γ momentum; $\vec{k}$ is the relative momentum, in the center of mass of the recoiling nucleus, of the fragments whose reduced mass is μ; m_π is the mass of the pion; and $\varphi_\pi(\vec{r})$ is the initial bound-state pion wave function. The constant $\alpha=\frac{1}{137}$.

The operator in the space of the jth nucleon,

$$O_j=\vec{\epsilon}_\lambda^{\,*}e^{-i\vec{q}\cdot\vec{r}_j}\varphi_\pi(\vec{r}_j)\,, \tag{4}$$

can be expanded in a multipole expansion by working in the order $[(\vec{l}_\gamma\times\vec{l}_\pi)_l\times\vec{\epsilon}_\lambda^{\,*}]_J$:

$$O_j=-\sum_{\substack{l_\gamma l_\pi l J\\ m_\pi\lambda}}(-i)^{l_\gamma}\hat{l}_\gamma{}^2\hat{l}_\pi\hat{l}^{-1}(l_\gamma 0 l_\pi 0\,|\,l0)(l_\gamma 0 l_\pi m_\pi|\,l m_\pi)(l m_\pi 1-\lambda\,|\,JM)D^J_{M'M}(\varphi_q,\theta_q,-\varphi_q)\vec{Y}^{M'}_{Jl}(\hat{r}_j)j_l(qr_j)R_{nl_\pi}(r_j)\,. \tag{5}$$

The angles the photon makes with the emitted-particle direction are (φ_q,θ_q); $j_l(qr)$ is the Bessel function coming from the photon; and $R_{nl_\pi}(r_j)$ is the radial wave function of the pion.

The multiple-scattering corrections to the impulse approximation can be largely[2] taken into account by using for $R_{nl_\pi}(r)$ a solution to the Schrödinger equation in which the potential is the sum of an optical-model potential (repulsive for s states, attractive for p states) and a Coulomb potential due to an extended source. A further correction,[2] due to the absorption of the pion nonradiatively and the subsequent emission of a γ ray, is assumed to be small.

Since we are dealing with ^{4}He, the initial state has angular momentum zero. The final scattering state is expanded in terms of angular momentum states,

$$\psi_f^{(-)}\equiv\psi_{s\nu}^{(-)}=\sum_{Jl}(l0s\nu\,|\,J\nu)\Phi^{(-)}_{lsJ\nu}\,,\quad \Phi^{(-)}_{lsJ\nu}=\pi^{1/2}\mathcal{A}\sum_{\substack{l's'\\m'}}(l'm's'\nu-m'\,|\,J\nu)\hat{l}'i^{l'}\psi_{s'\nu-m'}Y^{m'}_{l'}(\Omega_4)S^J_{l's',ls}(r_4)\,. \tag{6}$$

The function $\psi_{s\nu-m}$ contains the spin and isospin states of all four nucleons and the space coordinates of three particles, and $S^J_{l's',ls}(r_4)$ is a function of the relative separation of the neutron and triton, which asymptotically takes the form

$$S^J_{l's',ls}(r)=O_l(kr_4)\delta_{l'l}-I_{l'}(kr_4)U^{J*}_{l's',ls}\,. \tag{7}$$

The functions O_l and I_l are the usual[10] outgoing and incoming spherical waves, $U^J_{l's',ls}$ is the collision matrix, and $\mathcal{A}$ is the antisymmetrizer.

Equations (6) and (7) exhibit our approximations with respect to the scattering wave function: (1) All channels except the $t+n$ are ignored; and (2) the $t+n$ wave functions are taken to be cluster-type functions. The first approximation is justified by the relatively large ratio of elastic to inelastic scattering at scattering energies most important in the radiative pion capture. This is reflected in the fact that $t+n$ and ^{3}He$+p$ phase-shift[11,12] fits have been restricted to real phase shifts. The second approximation is justified by the success of resonating-group calculations[13,14] for scattering of light nuclei.

We take the ground state of ^{4}He to be $(1s)^4$ so that the spin and isospin functions form an SU(4) singlet $\{1\}$. Because the $\tau^{(-)}\sigma_i$ operators are generators of the group SU(4), the excited states of ^{4}H are members of an SU(4) multiplet $\{15\}$. In particular, those members with $S=1$, $T=1$, $T_z=-1$ are excited. If we use Gaussian wave functions for the three- and four-body bound states we get, after carrying out the spin and isospin sums,

$$\begin{aligned}\frac{d^2\Lambda}{dq\,d\Omega}&=\frac{\alpha f^2}{4\pi}\,\frac{qk\mu}{2\pi^2 m_\pi{}^3}\,\hat{l}_\pi{}^{-2}\sum_{m_\pi s\nu\lambda}|M_{s\nu\lambda,m_\pi}|^2\,,\\ M_{s\nu\lambda,m_\pi}&=\sum_{l_\gamma lJ}\sum_{m's}(i)^{l+l_\gamma}(-1)^{l_\pi+m_\pi+s}d^J_{\nu M}(\theta_q)\hat{J}^2\hat{l}^2\hat{l}_\gamma{}^2\hat{l}_\pi\begin{pmatrix}l_\gamma & l & l_\pi\\ 0 & 0 & 0\end{pmatrix}\begin{pmatrix}l_\gamma & l & l_\pi\\ 0 & -m_\pi & m_\pi\end{pmatrix}\begin{pmatrix}J & l & s\\ -\nu & 0 & \nu\end{pmatrix}\begin{pmatrix}J & l & 1\\ -M & m_\pi & -\lambda\end{pmatrix}\\ &\quad\times[I(l_\gamma n_\pi l_\pi lsJ)-K(l_\gamma n_\pi l_\pi lsJ)]\,.\end{aligned} \tag{8}$$

The direct and exchange integrals over the radial wave functions take the form:

$$
\begin{aligned}
I(l_\gamma n_\pi l_\pi l sJ) &= N\int d\vec{\rho}_1 d\vec{\rho}_2 d\vec{\rho}_3 \exp[-\mu_3(\tfrac{3}{2}\rho_1^2+2\rho_2^2)]\exp[-\mu_4(2\rho_1^2+\tfrac{8}{3}\rho_2^2+3\rho_3^2)] \\
&\quad\times S^J_{l1,\,ls}(\rho_3)R_{n_\pi l_\pi}(\tfrac{3}{4}\rho_3)j_{l_\gamma}(\tfrac{3}{4}q\rho_3)\,|\,Y_{l0}(\hat{\rho}_3)|^2\,, \\
K(l_\gamma n_\pi l_\pi lsJ) &= N\int d\vec{\rho}_1 d\vec{\rho}_2 d\vec{\rho}_3 \exp[-\mu_3(6\rho_1^2+\tfrac{1}{2}\rho_2^2+\tfrac{9}{32}\rho_3^2+\tfrac{3}{4}\vec{\rho}_2\cdot\vec{\rho}_3)]\exp[-\mu_4(8\rho_1^2+\tfrac{2}{3}\rho_2^2+\tfrac{27}{8}\rho_3^2+\vec{\rho}_1\cdot\vec{\rho}_3)] \\
&\quad\times S^J_{l1,\,ls}(\rho_3)R_{n_\pi l_\pi}(\tfrac{1}{3}\rho_2)j_l(\tfrac{1}{3}q\rho_2)Y_{l0}(\hat{\rho}_2)Y_{l0}(\hat{\rho}_3)\,.
\end{aligned}
\tag{9}
$$

The number of angular momenta couplings are the same as in the absorption of a γ ray by a nucleus of arbitrary spin leading to a continuum state. Thus, the m sum can be carried out in the usual way. However, we preferred to evaluate each $M_{sv\lambda,\,m_\pi}$ and perform the m sums numerically. One then gets a numerical angular distribution but not the expansion coefficients of a Legendre polynomial sum.

III. PION AND FINAL-STATE WAVE FUNCTIONS

The pion radial wave function $R_{nl\pi}(r)$ was obtained by solving the Schrödinger equation with a potential that is the sum of the Coulomb potential due to a uniformly charged sphere of radius 2.08 F and a repulsive (for s states) square-well optical potential of the same radius.[15] The real and imaginary well depths were adjusted to yield the observed $1s$ energy. The only known measurements[16] give the result that the energy shift, $\Delta E = \Delta E_R + i\Delta E_I$, compared with the Bohr energy level for a point nucleon is

$$
\begin{aligned}
\Delta E_R &= 89 \pm 60\ \text{eV}\,, \\
\Delta E_I &= \ \ 0 \pm 86\ \text{eV}\,.
\end{aligned}
\tag{10}
$$

(The vacuum polarization shift has been taken account of in the above numbers.) Because of their inability to measure a width, we took the old result of Bruckner,[17] $\Delta E_I = 54^{+45}_{-54}$ eV. Then the potential depths came out to be

$$
\begin{aligned}
V_R &= 7.9^{+5.7}_{-5.6}\ \text{MeV}\,, \\
V_I &= -5.1^{+3.0}_{-5.1}\ \text{MeV}\,.
\end{aligned}
\tag{11}
$$

For the central values we find that the probability of the $1s$ pion being within the nucleus is reduced by 23% as compared to the $1s$ Bohr orbit. We also found that the over-all rate is only changed by about 1% if an average $\overline{\varphi}_{1s}$ is extracted from the integrals as compared to leaving the complete function within the integral. Because of the large centripetal barrier for p states, we used Bohr orbits in this case.

The final scattering state must be treated with care, because for a given relative orbital angular momentum the amplitudes for channel spin 1 and 0 are coupled for $J=l$. The collision matrix $\underline{U}^*$ [from Eq. (7)] is first written in terms of eigenphases $\underline{\Delta}$:

$$\underline{U}^* = \underline{T}e^{-2i\underline{\Delta}}\underline{T}^{-1}\,, \tag{12}$$

where $e^{-2i\underline{\Delta}}$ is a diagonal matrix in channel space, each eigenphase $\underline{\Delta}_i$ being real, and $\underline{T}$ is a real orthogonal matrix. Then the scattering solution for a given J, with the incoming wave boundary condition, is

$$\underline{\psi}_J^{(-)} = -\tfrac{1}{2}i(\underline{O} - \underline{I}\,\underline{U}^*)\,, \tag{13}$$

where $\underline{I}$ and $\underline{O}$ are also treated as diagonal matrices. The solution $\underline{\psi}_J$ is a matrix where the ith column represents the asymptotic solution with unit outgoing flux in the ith channel. $\underline{\psi}_J^{(-)}$ can also be expanded in terms of standing waves,

$$
\begin{aligned}
\underline{\psi}_J^{(-)} &= -\tfrac{1}{2}i\,\underline{\Phi}e^{-i\underline{\Delta}}\underline{T}^{-1}e^{-i\underline{\omega}}\,, \\
\underline{\Phi} &= (\underline{F}\,\underline{T}\cos\underline{\Delta} + \underline{G}\,\underline{T}\sin\underline{\Delta})\,,
\end{aligned}
\tag{14}
$$

where $\underline{F}$ and $\underline{G}$ are the regular and irregular real asymptotic solutions and the $\underline{\omega}$ are the Coulomb phases for charged channels. The columns of the matrix $\underline{\Phi}$ are the so-called eigenphase solutions because the phase shift is the same for each channel.

In our specific case we have only one particle channel so the relative energies are the same for all channels. Then $\underline{F}$ and $\underline{G}$ are multiples of the unit matrix and

$$\underline{\Phi} = \underline{T}(\underline{F}\cos\underline{\Delta} + \underline{G}\sin\underline{\Delta})\,. \tag{15}$$

The coupled Schrödinger equation

$$(\underline{K} - \underline{E} + \underline{V})\underline{\Phi} = 0 \tag{16a}$$

is then simply diagonalized by $\underline{T}$:

$$\underline{V}_d = \underline{T}\,\underline{V}\,\underline{T}^{-1}\,, \quad \underline{\Phi} = \underline{T}\,\underline{\Phi}_d\,; \tag{16b}$$

and one can represent the scattering wave function in the internal region by introducing a set of diagonal potentials of the same shape but different depths which reproduce the set of eigenphases Δ_i.

TABLE I. Neutron square wells for $L = 1$. The parameters below reproduce the phase shifts of Ref. 11 and agree closely with the eigenphases from Ref. 12 obtained from a phase-shift analysis of ^{3}He(p, p). The potentials for the 1^- eigenchannels can be labeled by S only in the limit $\epsilon \to 0$, where ϵ is the mixing parameter.

	Channel spin	Depth (MeV)	Range (F)
1^-	0	4.7	4.2
1^-	1	7.0	4.2
2^-	1	13.4	3.5
0^-	1	3.1	4.0

The work of Tombrello[11] and McSherry and Baker[12] indicates that large positive phase shifts occur only in the 2^-, 1^-, and 0^- p-wave channels. Of these, it is the 1^- channel where $S = 0$ and $S = 1$ coupling occurs. The ^3S phase shift is essentially hard sphere with a hard-sphere radius. $A_c = 3.3$ F. The more recent work[12] on ^{3}He(p, p) reveals that the ^3D_J phase shifts are all small.

Our approximations for the radial wave functions, $S^J_{l' s', 1s}$, within the range of focus are the following: (1) For the $^3S_1$, $S^1_{01,01} = 0$ for $r \leq 3.3$ F. (2) The p-wave functions were determined by solving the radial Schrödinger equation with the square-well potentials shown in Table I. For the two-channel 1^- case,

$$T = \begin{pmatrix} \cos\epsilon & -\sin\epsilon \\ \sin\epsilon & \cos\epsilon \end{pmatrix}, \qquad (17)$$

and two values of ϵ were used, $\epsilon = -17°$, corresponding to the ^{3}He(p, p) phase-shift result,[12] and $\epsilon = -51°$ which is consistent with shell-model calculations,[18,19] that show roughly even mixtures of $^3P_1$ and $^1P_1$ in the $T = 1$ states. (3) The ^3D_J and higher states were represented by spherical Bessel functions $j_l(kr)$. In the asymptotic range the radial wave functions are, of course, determined by the observed phase shifts.

IV. RESULTS

The negative-parity partial waves dominate both 1s and 2p radiative capture. The curves in Fig. 1 show that for both 1s and 2p the γ-ray spectrum peaks at about 112 MeV. The spectrum for 1s capture falls off more rapidly with decreasing γ energy because the photon is in an $M1$ or $E2$ state rather than an $E1$ as for 2p capture. (Figure 2 exhibits the angular momentum couplings.) The theoretical 1s curve, folded for experimental resolution,[20] is compared with the experimental spectrum[4] in Fig. 3. The absolute magnitude is in fair agreement with the experimental differential capture rate (which rate, however, entails the assumption that all radiative and nonradiative captures occur from the 1s state), as well as that obtained from a simple shell-model estimate of the total rate.[4]

The angular distribution of the neutron (in the c.m. system of ^{4}H) with respect to the γ direction is shown in Fig. 4 for the peak γ energy of 112 MeV and in Fig. 5 for a much lower γ energy of 80 MeV. The backward-peaking characteristic of simple proton pole models is beginning to appear at this energy. The angular distribution is essentially the same for the alternate choice for the 1^- mixing angle ϵ.

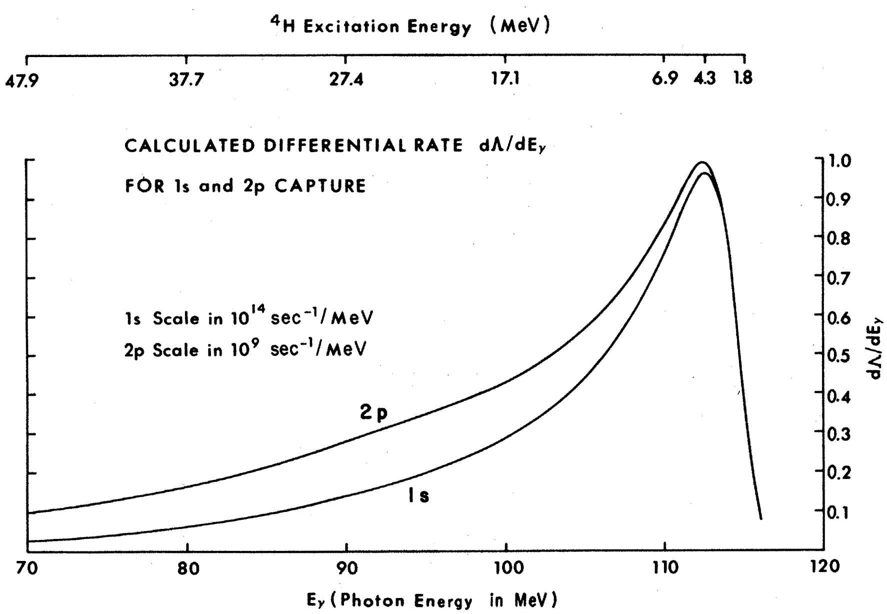

FIG. 1. Calculated 1s and 2p capture rates as a function of γ energy.

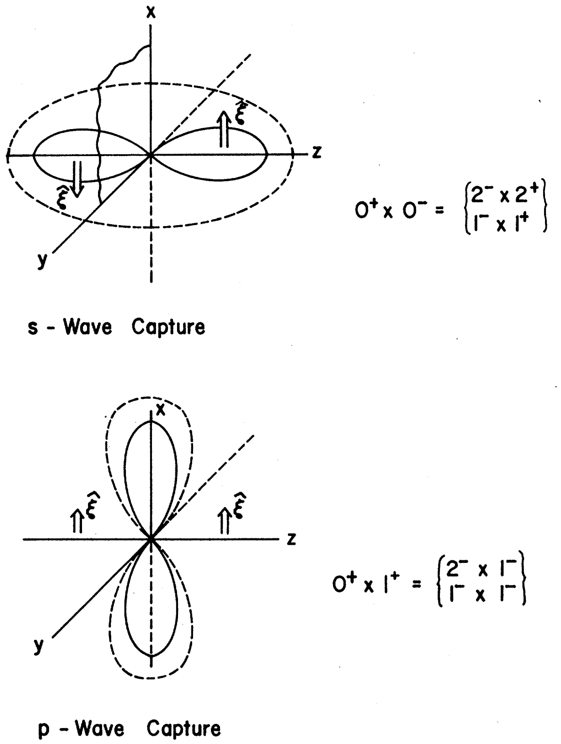

FIG. 2. A pictorial representation of the pion wave function (dashed line), the neutron wave function (solid curve), and the A field of the photon which is taken to be emitted in the z direction (polarization vectors are shown). The equations give the initial and final angular momentum couplings with the first number in each pair being the nuclear state, the second the boson state. One sees that for s-wave capture one gets overlapping neutron and photon "lobes" for forward and backward neutron emission, while for p-wave capture the pion and neutron lobes can overlap for 90° emission.

The difference between the $1s$ and $2p$ angular distribution is most evident at the peak energy. The distribution peaks at 0 and π for $1s$ capture (or any ns capture) but at $\frac{1}{2}\pi$ for $2p$. This characteristic difference is easily understood in terms of the angular momenta of the nuclear states and of the angular momenta of the initial and final boson states. Figure 2 illustrates the point.

We have defined two ratios in Eq. (2). A third ratio that is more directly observable is the ratio of radiatively captured pions to nonradiatively captured ones:

$$R_0 = \sum_n \left[\frac{\Lambda_\gamma(np)}{\Lambda(np)} w_{np} + \frac{\Lambda_\gamma(ns)}{\Lambda(ns)} w_{ns} \right] . \qquad (18)$$

Most models[5] of both processes show that the s-state capture rates are proportional to $|\varphi_{ns}(0)|^2$. Hence to a good approximation

$$\Lambda_\gamma(ns)/\Lambda(ns) = \Lambda_\gamma(1s)/\Lambda(1s) . \qquad (19)$$

The same relationship does not hold for $\Lambda_\gamma(np)/\Lambda(np)$, since the nonradiative rate,[21]

$$\Lambda(nl) = A_1 \int d\vec{r}\, \rho_N{}^2(r) |\varphi_{nl}(r)|^2 + A_2 \int d\vec{r}\, \rho_N{}^2(r) |\vec{\nabla}\varphi_{nl}(r)|^2 , \qquad (20)$$

depends on n for fixed l in a different way than does $\Lambda_\gamma(nl)$ for which the p-state pion-nucleon interaction is negligible. In the absence of detailed knowledge of $w(np)$ we make the assumption (justified only if the bulk of p-wave absorptions occur for the $2p$ orbital)

$$\Lambda_\gamma(np)/\Lambda(np) \cong \Lambda_\gamma(2p)/\Lambda(2p) . \qquad (21)$$

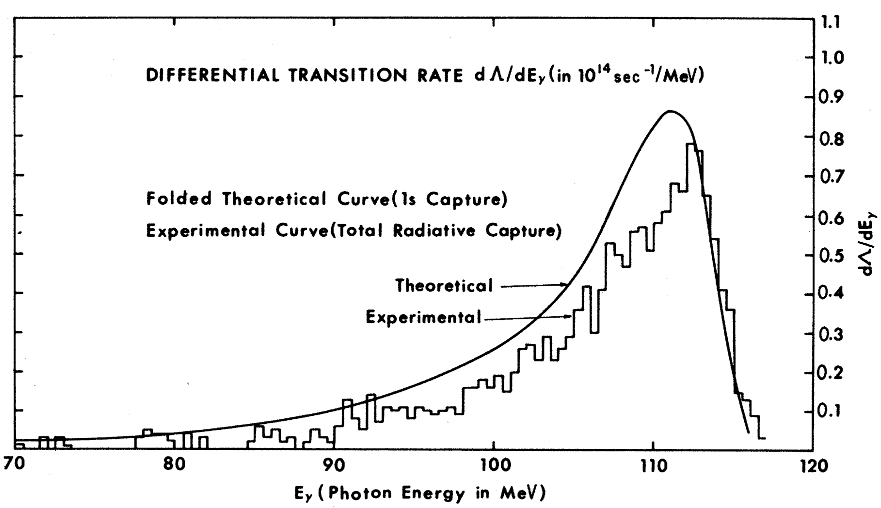

FIG. 3. Comparison of theoretical $1s$ curve [with experimental resolution folded in (Ref. 20)] and experimental spectrum. No renormalization has been attempted.

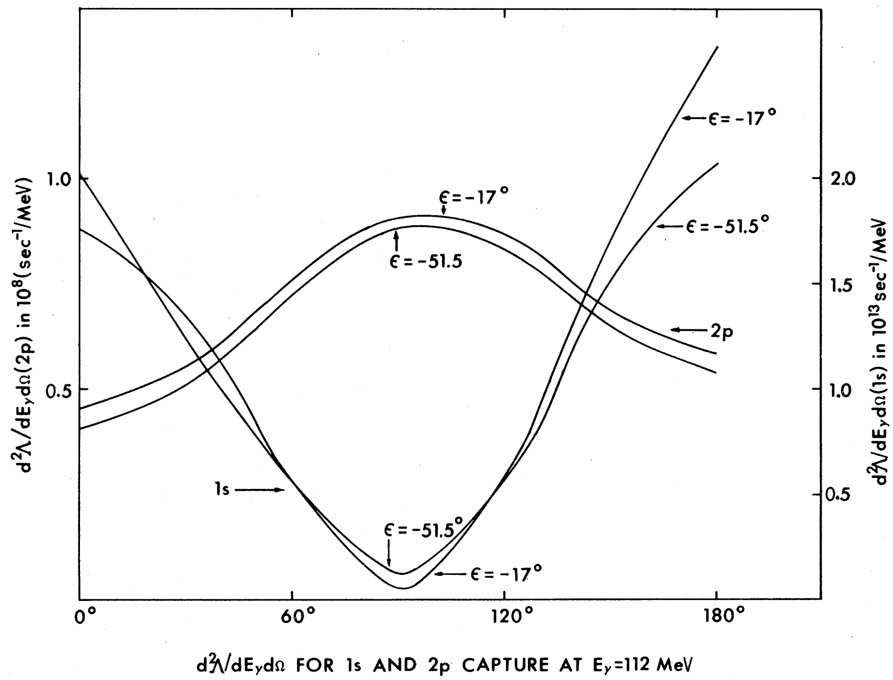

FIG. 4. Angular correlation of the neutron with respect to the γ ray at the peak in the spectrum for 1s and 2p capture.

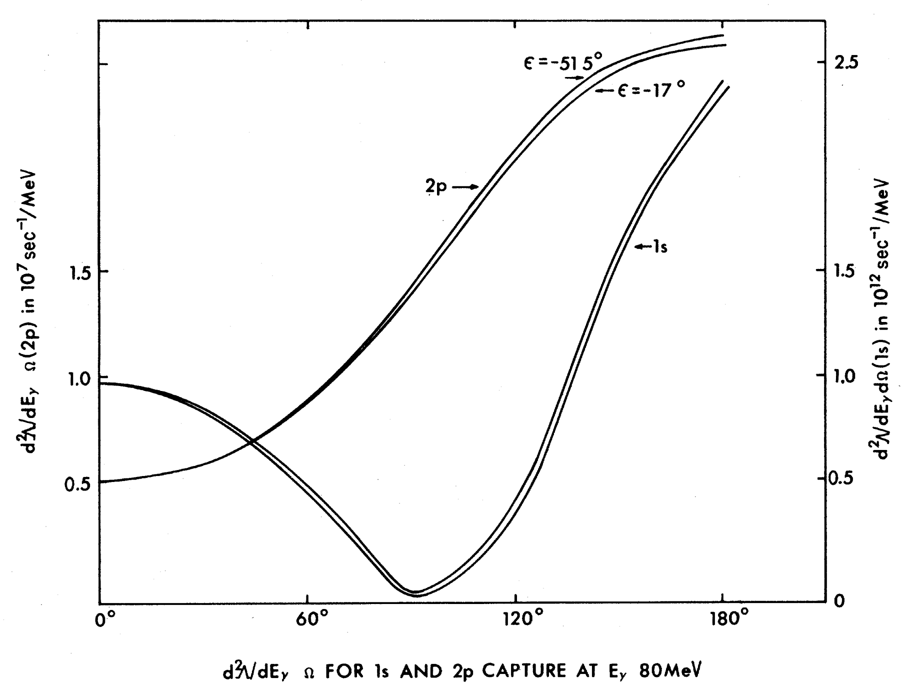

FIG. 5. Angular correlation of the neutron with respect to the γ ray at $E_\gamma = 80$ MeV. Once again 1s and 2p captures have been considered.

Integrating under our curves in Fig. 1 we get

$$\Lambda_\gamma(1s) = 1.3\times 10^{15}\ \text{sec}^{-1}, \quad \Lambda_\gamma(2p) = 1.8\times 10^{10}\ \text{sec}^{-1}. \tag{22}$$

The measured values of the total absorption rates from these orbitals[9] and for the ratio[22] $R(p/s)$ are

$$\Lambda(1s) = 3.1\pm 1.2\times 10^{16}\ \text{sec}^{-1}, \quad \Lambda(2p) = 5\pm 2\times 10^{12}\ \text{sec}^{-1}, \quad R(p/s) = 1.2\pm 0.3. \tag{23}$$

The ratio R_0 then comes out to be

$$R_0 = \frac{1}{1+R(p/s)}\left[\frac{\Lambda_\gamma(2p)}{\Lambda(2p)}R\left(\frac{p}{s}\right)+\frac{\Lambda_\gamma(1s)}{\Lambda(1s)}\right] = 2.1\pm 0.7\times 10^{-2}. \tag{24}$$

The observed ratio[4] is $1.28\pm 0.13\times 10^{-2}$ within the limits of our derived R_0.

The predicted value for $R_\gamma(p/s)$, which can be measured from an (n,γ) correlation experiment, turns out to be

$$R_\gamma(p/s) = 0.1\pm 0.05. \tag{25}$$

A comparison with an earlier paper on the same subject[4] illustrates, at the very least, the fact that better x-ray cascade measurements and interpretations thereof must be carried out to lower the range of error in the theoretical estimate. In the earlier paper the rate was calculated for $1s$ capture only using shell-model wave functions, and the continuum nature of the final states was taken into account by using a Lorentz factor to spread the states. The total capture rate from the $1s$ orbit was taken to be $\Lambda(1s) = 5.5\times 10^{16}\ \text{sec}^{-1}$, an extrapolation from heavier-element measurements.[23] The ratio given in Eq. (24) of radiative-to-nonradiative pion capture differs from Ref. 4 in three respects: (1) $\Lambda_\gamma(1s)$ in Eq. (22) is about 50% larger than the shell-model result; (2) both s- and p-wave capture have been considered in the present work; (3) the value for $\Lambda(1s)$ adopted in Eq. (23) is about 50% smaller than that given immediately above. The changes (1) and (3) raise the ratio R_0; change (2) tends to lower it, since p-wave radiative capture is relatively less important than p-wave nonradiative capture.

The values for $\Lambda_\gamma(ns)$ and $\Lambda_\gamma(np)$ would probably be lowered somewhat if a ground-state wave function which has an exponential g decay instead of a Gaussian dependence were used. Thompson has compared the spectrum[24] for $^4\text{He}(\gamma, d)\text{D}$ calculated with the same final-state continuum wave function but with either an exponential or Gaussian dependence for the ^{4}He ground state. He finds that with the exponential wave function the peak in the spectrum is narrower and shifts to a lower relative energy in the $d+d$ system compared to the Gaussian. A similar situation should obtain with respect to the $^3\text{H}+n$ final state, and Fig. 3 reveals that such a shift would give a more perfect fit to the observed spectrum.

In conclusion, we have improved the calculation presented in Ref. 4 by including the effect of p-state capture and by using continuum wave functions. The resulting ratio of radiative-to-nonradiative capture seems higher than experimentally observed but the large error bars preclude a definite conclusion. The calculation should be repeated with a better functional form for the ^{4}He ground state.

However, the ratio of $\Lambda_\gamma(2p)/\Lambda_\gamma(1s)$ should be relatively independent of the ground-state form, so our value of 0.1 ± 0.05 can be improved only by getting improved values of $\Lambda(1s)$, $\Lambda(2p)$, and $R(p/s)$. For the p-shell nuclei $R_\gamma(p/s)$ is harder to obtain because continuum phase shifts are not known. However, in these states there are many transitions to bound states that can be studied.

Note added in proof: In a recent article concerned with radiative pion capture in ^{12}C,[25] it is asserted that the terms linear in the photon and pion momenta should not be dropped from the photoproduction amplitude as we have done in Eq. (1), especially when treating p-state capture of the pion. This is in direct conflict with the findings of the authors of Ref. 1, so that more work must be done to resolve the issue.

†Work supported in part by Office of Naval Research.

[1] J. DeLorme and T. E. O. Ericson, Phys. Letters 21, 98 (1966).

[2] L. P. Fulcher, R. Guy, J. M. Eisenberg, and H. Pietschmann, Phys. Letters 29B, 338 (1969).

[3] M. Bander, Phys. Rev. 134, B1052 (1964).

[4] J. A. Bisterlich, K. M. Crowe, A. S. L. Parsons, P. Skarek, P. Truoel, and C. Werntz, Phys. Rev. Letters 25, 950 (1970).

[5] D. S. Koltun and A. Reitan, Nucl. Phys. B4, 629 (1968).

[6] D. S. Koltun and A. Reitan, Phys. Rev. 155, 1139 (1967).

[7] Y. Eisenberg and D. Kessler, Phys. Rev. 123, 1475 (1961).

[8] M. Ericson and A. Figereau, Nucl. Phys. B3, 609 (1967).

[9] S. Berezin, G. Burleson, D. Eartly, A. Roberts, and T. O. White, Nucl. Phys. B16, 389 (1970).

[10]A. M. Lane and R. G. Thomas, Rev. Mod. Phys. 30, 257 (1958).
[11]T. A. Tombrello, Phys. Rev. 143, 609 (1966).
[12]D. H. McSherry and S. D. Baker, Phys. Rev. C 1, 888 (1970).
[13]P. Szydlik and C. Werntz, Phys. Rev. 138, B866 (1964).
[14]B. H. Bransden, H. H. Robertson, and P. Swan, Proc. Phys. Soc. (London) 69A, 601 (1956).
[15]R. Seki and Z. Cromer, Phys. Rev. 156, 93 (1967).
[16]R. Wetmore, D. Buckle, J. Kane, and R. Siegel, Phys. Rev. Letters 19, 1003 (1967).
[17]K. A. Brueckner, Phys. Rev. 98, 769 (1955).
[18]B. R. Barrett, Phys. Rev. 154, 955 (1966).
[19]G. Sh. Gogsadze and T. I. Kopsleishvili, Yadern. Fiz. 8, 875 (1968) [transl.: Soviet J. Nucl. Phys. 8, 509 (1969)].
[20]The instrumental resolution function for this experiment was kindly supplied to us by Dr. P. Truoel.
[21]M. Ericson and T. E. O. Ericson, Ann. Phys. (N.Y.) 36, 323 (1966).
[22]S. Berezin, G. Burleson, D. Eartly, A. Roberts, and T. O. White, Phys. Letters 30B, 27 (1969).
[23]D. Jenkins and R. Kunselman, Phys. Rev. Letters 17, 1148 (1968).
[24]D. R. Thompson, Nucl. Phys. A154, 442 (1970).
[25]S. Skupsky, Phys. Letters 36B, 271 (1971).

PHYSICAL REVIEW C VOLUME 4, NUMBER 6 DECEMBER 1971

Clustering Characteristics of ^{6}Li from the ^{6}Li$(\alpha,\alpha x)Y$ Reaction at $E_\alpha = 50$ MeV

J. M. Lambert,* R. J. Kane,† P. A. Treado,* L. A. Beach, E. L. Petersen, and R. B. Theus
U. S. Naval Research Laboratory, Washington, D. C. 20390

(Received 19 August 1971)

The quasielastic scattering of 50-MeV α particles has been used as a tool to study the cluster configurations of the ^{6}Li nucleus by means of the ^{6}Li$(\alpha, \alpha x)Y$ reaction. Data have been obtained in kinematically complete experiments and at exact quasielastic angles for those cases corresponding to $x = p$, d, t, ^{3}He, and α. Analysis has been carried out in the framework of the plane-wave impulse approximation. Quasielastic cross sections have been measured and experimental momentum distributions extracted. Theoretical fits to these distributions using simple Gaussian and exponential functions have been calculated and used to determine both absolute and relative clustering probabilities with fair success. The more reliable relative probabilities indicate strong p, d, and α clustering in ^{6}Li and rather weak t and ^{3}He clustering.

I. INTRODUCTION

Multiparticle-breakup (MPB) reaction studies have expanded substantially in recent years and have provided a useful method of investigating nuclear structure and reactions.[1-3] Present detection and analysis techniques identify particles and record coincident energy information for numerous outgoing channels in kinematically complete experiments involving more than two particles in the final state. For relatively low bombarding energies, this type of experiment has been shown to proceed by sequential-decay processes through definite states of particle-unstable systems.[4-7] For moderate bombarding energies, the "quasielastic" (QE) process has been observed and studied.[8-10] In this process, it is assumed that the target nucleus has a structure consisting of identifiable nucleons and/or clusters of nucleons, and that the nucleons or clusters can be knocked out of the system in a manner that can be described in terms of elastic scattering of the incident particle and the product particle or cluster. Reactions such as $(p, 2p)$, $(\alpha, 2\alpha)$, and $(p, p\alpha)$ typify this process.

The techniques of MPB, in general, and QE scattering, in particular, should be very useful for investigating questions relating to the cluster and shell models of nuclei, even though the interpretation of such experiments is difficult and still debated.[11] Some of the early QE experiments suggested that in the $(p, 2p)$ process it was possible to knock out protons with different binding energies that were interpreted as being associated with different shells of the nucleus.[12,13] In addition, angular-distribution studies indicated that angular momentum information about the target nucleus could be obtained.[14,15] This information suggested that the shell model may not be valid for the ^{6}Li nucleus.[16] Previous experiments have investigated a given QE process, for example $(\alpha, 2\alpha)$, using various targets to determine the validity of the assumptions used in the analysis of such experiments. The validity of the plane-wave impulse approximation[17] (PWIA), the use of a modified cutoff approximation,[18] the separa-